

Four-point resistance of individual single-wall carbon nanotubes

B. Gao,¹ Y.F. Chen,² M.S. Fuhrer,² D.C. Glattli,^{1,3} A. Bachtold^{1*}

¹ *Laboratoire Pierre Aigrain, Ecole Normale Supérieure, 24 rue Lhomond, 75231 Paris 05, France.* ² *Department of Physics and Center for Superconductivity Research, University of Maryland, College Park, Maryland 20742, USA.* ³ *SPEC, CEA Saclay, F-91191 Gif-sur-Yvette, France.*

(Dated: July 14, 2018)

We have studied the resistance of single-wall carbon nanotubes measured in a four-point configuration with noninvasive voltage electrodes. The voltage drop is detected using multiwalled carbon nanotubes while the current is injected through nanofabricated Au electrodes. The resistance at room temperature is shown to be linear with the length as expected for a classical resistor. This changes at cryogenic temperature; the four-point resistance then depends on the resistance at the Au-tube interfaces and can even become negative due to quantum-interference effects.

PACS numbers: 73.63.Fg, 72.80.Rj, 72.15.Lh, 73.23.-b

Transport measurements are a powerful technique to investigate electronic properties of molecular systems [1]. Most often, individual molecular systems are electrically attached to two nanofabricated electrodes. However, such two-point experiments do not allow the determination of the intrinsic resistance that results from scattering processes involving e.g. phonons or disorder. Indeed, the resistance is mainly dominated by poorly defined contacts that lie in series. A solution to eliminate the contribution of contacts has been found with scanning probe microscopy techniques [2, 3, 4, 5, 6], which enable the measurement of resistance variations along long systems such as nanotubes, but these techniques have only been applied at room temperature. The standard method to determine the intrinsic resistivity of macroscopic systems is the four-point measurement. The application of this technique to molecular systems is challenging however, since the electrodes used so far have been invasive. For example, nanofabricated electrodes were shown to divide nanotubes into multiple quantum dots [7].

We report four-point resistance measurements on single-wall carbon nanotubes (SWNT) using multiwalled carbon nanotubes (MWNT) as noninvasive voltage electrodes (Fig. 1(a)). We find that SWNTs are remarkably good one-dimensional conductors with resistances as low as 1.5 k Ω for a 95 nm long section. The nanotube resistance is shown to linearly increase with length at room temperature, in agreement with Ohm's law. At low temperature, however, the resistance can become negative and the amplitude then depends on the resistance at the Au-SWNT interfaces. In this regime, four-point measurements can be described by the Landauer-Büttiker formalism taking into account quantum-interference effects.

Before discussing these measurements, we briefly review the basic physics of four-point measurements (Fig. 1(b)). In the diffusive incoherent limit, the four-point resistance R_{4pt} of SWNTs, characterized by 4 conducting channels, is given by [8]

$$R_{4pt} = \frac{h}{4e^2} \frac{L}{l_e} \quad (1)$$

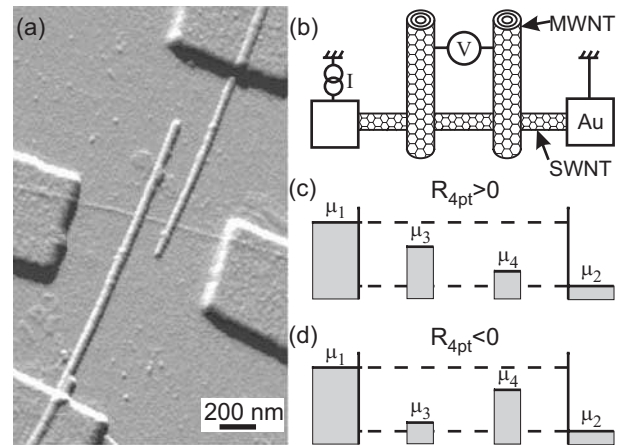


FIG. 1: (a) Atomic force microscopy image of a SWNT contacted by 2 MWNTs and 2 Au electrodes. (b) Schematic of the R_{4pt} measurement. R_{4pt} is measured in the linear regime with eIR_{2pt} below kT . (c,d) Levels of the electrochemical potential for the 4 electrodes that give a positive R_{4pt} in (c) and a negative R_{4pt} in (d).

with l_e the elastic mean-free path and L the separation between the voltage electrodes. Equation 1 describes the intrinsic resistance generated by the electronic backscattering along the nanotube.

We next remind how R_{4pt} can deviate from equation 1. The transmission to the voltage electrodes should be made weak to suppress an additional resistance contribution that results from electrons entering the voltage electrodes. Such electrons are replaced by electrons that scatter into either direction of the tube, enhancing the resistance [9].

By introducing quantum-interference effects, four-point measurements can give striking results such as negative R_{4pt} . This is best seen using the Büttiker formula [10, 11, 12], which is convenient for the description of multi-terminal conductors. The current I_α in each electrode is related to the electrochemical potential μ_β of

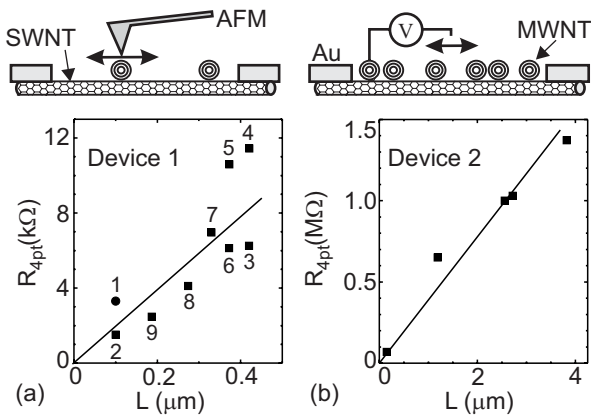


FIG. 2: Length dependence of R_{4pt} at room temperature and $V_g = 0$. (a) SWNT contacted by 2 MWNTs. One MWNT is displaced back and forth with an AFM tip. Points are numbered to describe the measurement sequence. Point 1 has been acquired one week before in the cryostat. (b) SWNT contacted by 6 MWNTs.

other electrodes by

$$I_\alpha = \frac{4e^2}{h} \sum_\beta T_{\beta\alpha} \mu_\alpha - T_{\alpha\beta} \mu_\beta \quad (2)$$

with $T_{\alpha\beta}$ the total transmission between the α and the β electrodes (Fig. 1(c,d)). The condition $I_3 = 0$ for a voltage probe gives $\mu_3 = (T_{31}\mu_1 + T_{32}\mu_2)/(T_{31} + T_{32})$. The transmission between electrodes 3 and 4 has been neglected since it corresponds to a second-order process. The potential of the voltage electrode μ_3 can thus take any value between μ_1 and μ_2 . Since the same holds for μ_4 , R_{4pt} can be negative (see Fig. 1(c,d)). Using $R_{2pt} = (\mu_1 - \mu_2)/I$ and $R_{4pt} = (\mu_3 - \mu_4)/I$, we find that R_{4pt} takes any value between [11]

$$-R_{2pt} \leq R_{4pt} \leq R_{2pt} \quad (3)$$

Previous work on ballistic one-dimensional conductors fabricated in semiconductors showed that R_{4pt} can become slightly negative [13, 14, 15]. However, large negative modulations of R_{4pt} remain to be observed.

We have fabricated nanotube circuits with a new layout for four-point measurements. First, ~ 1 nm diameter SWNTs grown by laser-ablation [16] or chemical-vapor deposition [17] are selected with an atomic force microscopy (AFM). Voltage electrodes are then defined by positioning two MWNTs above the SWNT using AFM manipulation. We choose such voltage electrodes since the electric transmission between two nanotubes is known to be low [18, 19]. Then, Cr/Au electrodes are patterned for electric connection with standard electron-beam lithography techniques (see Fig. 1(a)).

We now look to the length dependence of R_{4pt} measured at 300K. Fig. 2(a,b) shows that R_{4pt} linearly increases with the length, in agreement with Ohm's law and eq. 1. Two types of measurements have been carried. In

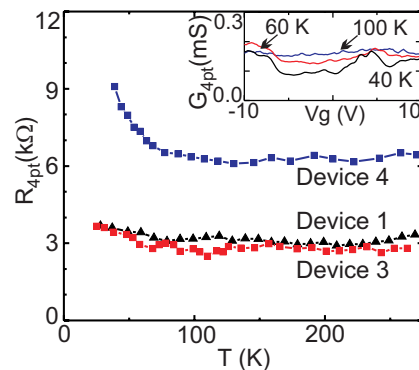


FIG. 3: Temperature dependence of R_{4pt} measured at zero V_g . The inset shows G_{4pt} as a function of V_g for Device 4.

Fig. 2(b), 6 MWNTs have been placed on a long SWNT, enabling the resistance measurement of multiple portions [20]. In Fig. 2(a), an AFM tip has been used to change the separation between two MWNTs. Most points have been recorded while decreasing L , so that the resistance enhancement with the length is not due to a structural degradation during the manipulation. However, the manipulation might well stretch the tube, deposit or remove some molecules adsorbed on the SWNT, or modify the pressure applied by the MWNT on the SWNT. Those modifications may account for the scattered R_{4pt} points in Fig. 2(a).

The measurements above also show that R_{4pt} tends to zero as the length is reduced. This suggests no (or little) additional contribution to the resistance from the MWNT contacts. Our device layout thus allows for the first direct measurement of the intrinsic resistance of a nanotube. The lowest resistance that we obtained is 1.5 k Ω for a 95 nm long section (Fig. 2(a)). Such a low resistance is remarkable, since the resistance of quasi one-dimensional conductors is expected to be dramatically enhanced with the presence of disorder or phonons. This agrees with previous two-point measurements [21, 22, 23, 24] since R_{2pt} was shown to approach the quantum resistance $h/4e^2 = 6.5$ k Ω , which suggests low intrinsic resistance.

Further insight into transport properties is obtained by decreasing the temperature T . Figure 3 shows that R_{4pt} does not change for T above ~ 80 K, suggesting that the intrinsic resistance is related to some static disorder and not to phonons. At lower T , however, the inset of Fig. 3 shows that G_{4pt} fluctuates with sweeping of the backgate voltage V_g .

We now discuss the possible origin of these fluctuations. They may originate from low-transmission barriers created by the MWNTs or some static disorder that form quantum dots along the tube. The transport may then be dominated by Coulomb blockade (CB). However, the conduction stays mostly constant with T above $T^* \sim 60$ K, the temperature at which fluctuations appear. This is in opposition to CB theory [25] that predicts

	R_{4pt} (k Ω)	L (nm)	l_e (nm)	T^* (K)	L_T (nm)	
Device 1	3.3	95	185	~ 40	~ 150	CVD
	1.5	95	408			CVD
Device 2	37.0	100	17			LA
Device 3	2.7	150	358	~ 30	~ 200	CVD
Device 4	6.3	140	143	~ 60	~ 100	LA
Device 5	12.7	590	300	~ 30	~ 200	LA

TABLE I: Device characteristics. The first line of Device 1 corresponds to properties measured in the cryostat and the second to that measured one week later during AFM manipulation. Values of Device 2 are extracted from the linear fit in Fig. 2(b). All SWNTs are metallic except Device 1 and 2. Device 1 is a small-gap semiconductor with the current reduction occurring at $V_g > 2$ V. Device 2 is a large-gap semiconductor with the threshold voltage at 40 V. LA = laser ablation. CVD = chemical vapor deposition.

$G = G_0(1 - \frac{1}{3}E_c/kT)$ for temperatures larger than the charging energy E_c , expected to be close to kT^* . Moreover, the best fit between this model and measurements above T^* gives $E_c/k \simeq 5$ K, which is much lower than T^* . Another mechanism is thus needed to account for the fluctuations

The presence of disorder is expected to generate a complicated interference pattern along the tube that should vary with the Fermi level. This results in aperiodic conductance fluctuations around the classical conductance when sweeping V_g [26], which is consistent with our measurements. Such fluctuations appear when effects of thermal averaging and phase decoherence are weak enough so that the thermal length $L_T = \hbar v_F/kT$ and the coherence length L_φ are larger than the elastic mean-free path. Interestingly, L_T at $T^* = 60$ K is comparable to l_e that is determined using Eq. 1 (see Table 1). This suggests that thermal averaging is here at least as detrimental as decoherence. Note, moreover, that the amplitude of the fluctuations approaches e^2/h at ~ 40 K. This is expected [26] when the lower of L_T and L_φ is comparable to the separation between the voltage electrodes, which is again consistent with measurements since $L_T = 150$ nm and $L = 140$ nm. Overall, our measurements suggest that quantum-interference effects start to modify the classical resistance given by eq. 1 around a few tens of Kelvin.

We turn now our attention to two-point measurements at the much lower temperature of 1.4 K. Figure 4(a) shows a series of CB peaks, which appear at the same gate voltages for measurements between different pairs of electrodes. This indicates that Au and MWNT electrodes probe the same nanotube quantum dot. The peak occurrence is quite regular with a spacing of $V_g \simeq 75$ mV. Coulomb diamonds measurements (not shown) give that the charging energy $E_c \approx 5$ meV. It has been shown that $E_c \approx \frac{5 \text{ meV}}{L[\mu\text{m}]}$ for similarly prepared samples [27], so that the dot length is $\sim 1 \mu\text{m}$, which is consistent with the 600 nm separation between Au electrodes. These measurements suggest that MWNTs are sufficiently noninvasive to not divide the SWNT in multiple quantum dots,

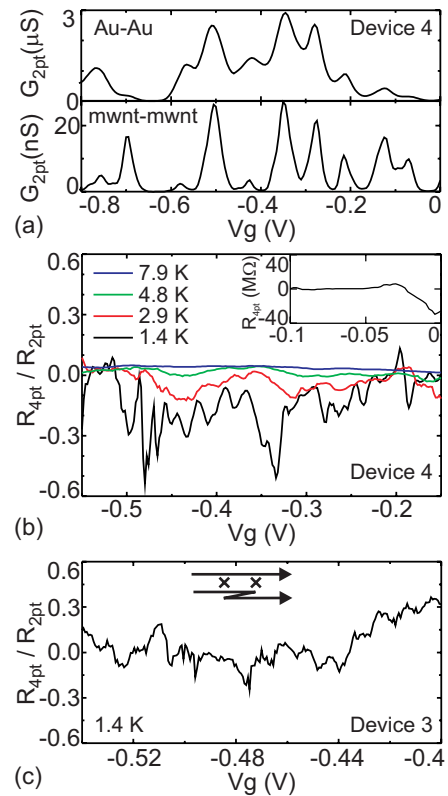


FIG. 4: Negative four-point resistance at low temperature. (a) Two-point conductance as a function of V_g at 1.4 K. R_{2pt} measured between Au electrodes is checked to be lower than R_{2pt} between MWNT electrodes in this V_g region. CB peaks measured between different electrodes appear also at the same V_g s for Device 1 and 3. (b,c) R_{4pt}/R_{2pt} as a function of V_g . The inset of (b) shows $R_{4pt}(V_g)$ at 1.4 K. Similar results are also obtained for Device 1. The inset of (c) shows two scattering centers that generate interference.

in opposition to nanofabricated electrodes [7].

Having shown that the SWNT is a single quantum dot over its length at 1.4 K, we now look at the four-point measurements. The inset of Fig. 4(b) shows that R_{4pt} becomes -29 M Ω near zero V_g . However, R_{4pt} significantly drops to 0 for V_g between -0.05 and -0.1 V when the two-point conductance between Au electrodes increases, in agreement with Eq. 3. Figures 4(b,c) show that the modulations of R_{4pt}/R_{2pt} are significant, with absolute values that reach as high as 0.6.

We now discuss the origin of the negative R_{4pt} . It could arise from voltage electrodes that differently couple to the left and the right moving states inside the tube [12, 13, 14]. However, such a classical effect should persist at higher temperature, which is not the case since R_{4pt} is only positive at $T \gtrsim 10$ K.

The resistance ratio R_{4pt}/R_{2pt} is given by [11]

$$\frac{R_{4pt}}{R_{2pt}} = \frac{T_{31}T_{42} - T_{32}T_{41}}{(T_{31} + T_{32})(T_{41} + T_{42})} \quad (4)$$

Part of the fluctuations are expected to come from

the Coulomb blockade observed at 1.4 K that leads to oscillations in T_{ij} transmissions. However, regular $V_g = 75\text{mV}$ CB oscillations cannot alone account for the rapid $V_g \sim 10\text{mV}$ fluctuations of R_{4pt}/R_{2pt} in Fig. 4(b). We rather attribute those fluctuations to quantum-interference terms [28, 29] that are contained in T_{ij} transmissions and that may arise from the superposition of different electronic paths between i and j electrodes [30]. Indeed, the disorder along the SWNT leads to different possibilities in the pathway between 2 electrodes (see the inset of Fig. 4(c)). It is also likely that the sign change originates from those interferences. Variations of T_{ij} transmissions with V_g are then uncorrelated, enabling the sign reversal of the numerator in Eq. 4.

R_{4pt}/R_{2pt} goes to zero when the temperature is increased to $\sim 5\text{K}$ (Fig. 4(b)). This is expected when the nanotube is no longer phase-coherent over its length, so that the quantum-interference term of the transmissions vanishes. Another possibility is that the quantum-interference term is washed out due to thermal averaging, since kT enhances the number of electron paths between two electrodes that contribute to transport. Interestingly, the 510 nm thermal length at 5K is comparable

to the 600 nm separation between Au electrodes of Device 4. L_T is $(\hbar v_F l_e / kT)^{1/2}$ since the transport is here diffusive. This points to the same finding observed at higher temperature that the thermal length apparently is the relevant parameter for quantum-interference phenomena in SWNTs.

In conclusion, we have shown that quantum-interference effects dramatically modulate the four-point resistance of SWNTs, so that R_{4pt} can even become negative. This happens when the thermal length is longer than the dimension of the system. The thermal length is 20 nm long at room temperature; hence it is likely that inclusion of these quantum-mechanical interference effects will ultimately be required in the design of practical multi-terminal intramolecular devices.

We thank C. Delalande for support, L. Forro for MWNTs, and R. Smalley for laser-ablation SWNTs. LPA is CNRS-UMR8551 associated to Paris 6 and 7. The research in Paris has been supported by ACN, Sesame. YFC and MSF acknowledge support from the U.S. National Science Foundation through grant DMR-0102950.

* corresponding author: bachtold@lpa.ens.fr

-
- [1] C. Joachim, J. K. Gimzewski, A. Aviram, *Nature* **408**, 541 (2000).
- [2] A. Bachtold, *et al.*, *Phys. Rev. Lett.* **84**, 6082 (2000).
- [3] P.J. de Pablo, *et al.*, *Phys. Rev. Lett.* **88**, 036804 (2002).
- [4] M. Freitag, *et al.*, *Phys. Rev. Lett.* **89**, 216801 (2002).
- [5] M.S. Gudixsen, *et al.*, *Nature* **415**, 617 (2002).
- [6] Y. Yaish, *et al.*, *Phys. Rev. Lett.* **92**, 046401 (2004).
- [7] A. Bezryadin, *et al.*, *Phys. Rev. Lett.* **80**, 4036 (1998).
- [8] Equation 1 is obtained from the Landauer formula $h/4e^2(1-T)/T$ with the transmission $T = l_e/(L + l_e)$. Alternatively, eq. 1 can be derived from the conductivity $\sigma = e^2 D \rho$ with the diffusion constant $D = v_F l_e$ and the density of states $\rho = 4/(\hbar v_F)$ for SWNTs.
- [9] For example, a transmission of 0.4 at the interfaces generates an additional resistance of around $0.1 h/4e^2$ by incoherently combining scattering matrices that describe backscattering along the tube and the coupling to the voltage electrodes (matrix (1) in M. Büttiker, *Phys. Rev. B* **32**, R1846 (1985)).
- [10] M. Büttiker, *Phys. Rev. Lett.* **57**, 1761 (1986).
- [11] M. Büttiker, *IBM J. Res. Develop.* **32**, 317 (1988).
- [12] S. Datta, *Electronic Transport in Mesoscopic Systems* (Cambridge University Press, Cambridge, 1997).
- [13] G. Timp, *et al.*, *Phys. Rev. Lett.* **60**, 2081 (1988).
- [14] Y. Takagaki, *et al.*, *Solid Stat Commun.* **68**, 1051 (1988).
- [15] R. de Picciotto, *et al.*, *Nature* **411**, 51 (2001).
- [16] A. Thess *et al.*, *Science* **273**, 483 (1996).
- [17] J.H. Hafner, *et al.*, *Phys. Chem. B* **105**, 743 (2001).
- [18] M.S. Fuhrer, *et al.*, *Science* **288**, 494 (2000).
- [19] B. Gao, *et al.*, *Phys. Rev. Lett.* **92**, 216804 (2004).
- [20] We checked that R_{4pt} at 300 K is independent of the contact resistance at the current electrodes by using different pairs of MWNT and Au electrodes for the current injection. R_{2pt} varied between 1.2 and 11 M Ω .
- [21] W. Liang, *et al.*, *Nature* **411**, 665 (2001).
- [22] J. Kong, *et al.*, *Phys. Rev. Lett.* **87**, 106801 (2001).
- [23] D. Mann, *et al.*, *Nano Lett.* **3**, 1541 (2003).
- [24] B. Babic and C. Schönenberger, *Phys. Rev. B* **70**, 195408 (2004).
- [25] P. Joyez, *et al.*, *Phys. Rev. Lett.* **79**, 1349 (1997).
- [26] C.W.J. Beenakker and H. Van Houten, *Solid State Phys.* **44**, 1 (1991).
- [27] M. Bockrath, *et al.*, *Science* **275**, 1922 (1997); D.H. Cobden, *et al.*, *Phys. Rev. Lett.* **81**, 681 (1998); J. Nygard, *et al.*, *Appl. Phys. A* **69**, 297 (1999).
- [28] V.A. Gopar, M. Martinez, P.A. Mello, *Phys. Rev. B* **50**, 2502 (1994).
- [29] M. Büttiker, *Phys. Rev. B* **40**, R3409 (1989).
- [30] Sweeping the magnetic field B induces fluctuations of R_{4pt} with the smallest fluctuations ≈ 6 T for Device 4. The corresponding Zeeman energy, which is 0.7 meV using the Landé factor $g = 2$, is consistent with the rapid $V_g \approx 10\text{mV}$ fluctuations in Fig. 4(b) since the coupling efficiency measured from Coulomb diamonds is $\alpha = 1/15$.